

Functional properties of a pore mutant in the *Drosophila melanogaster* inositol 1,4,5-trisphosphate receptor

Sonal Srikanth^{a,b}, Zhengnan Wang^b, Gaiti Hasan^a, Ilya Bezprozvanny^{b,*}

^aNational Centre for Biological Sciences, Tata Institute of Fundamental Research, Gandhi Krishi Vigyan Kendra Campus, Bangalore 560 065, India

^bDepartment of Physiology, University of Texas Southwestern Medical Center at Dallas, Dallas, TX 75390, USA

Received 8 July 2004; revised 19 August 2004; accepted 21 August 2004

Available online 8 September 2004

Edited by Maurice Montal

Abstract The inositol (1,4,5)-trisphosphate receptor (InsP₃R) is an intracellular calcium release channel that plays a crucial role in cell signaling. In *Drosophila melanogaster*, a single InsP₃R gene (*itpr*) encodes a protein (DmInsP₃R) that is ~60% conserved with mammalian InsP₃Rs. The functional properties of wild-type (WT) and mutant DmInsP₃Rs have recently been described [Srikanth et al., *Biophys. J.* 86 (2004) 3634–3646]. Here, we use the planar lipid bilayer reconstitution technique to describe single channel properties of a *ka901* point mutant (G2630S) in the pore-forming region of DmInsP₃R. We find that homomeric *ka901* channels are not functional, but the heteromeric WT:*ka901* mutant channels display increased conductance, longer channel open time and altered ion selectivity properties when compared to WT DmInsP₃R. Obtained results are consistent with the gain of function phenotype observed in *ka901/+* mutant flies.

© 2004 Published by Elsevier B.V. on behalf of the Federation of European Biochemical Societies.

Keywords: Inositol (1,4,5)-trisphosphate receptor; Structure–function; Planar lipid bilayer; Single channel recording; *Drosophila melanogaster*

1. Introduction

The inositol (1,4,5)-trisphosphate receptor (InsP₃R) is an intracellular calcium (Ca²⁺) release channel that plays a critical role in Ca²⁺ signaling [1]. The mammalian genome encodes three different isoforms of the InsP₃R-type I (InsP₃R1), type II (InsP₃R2) and type III (InsP₃R3) [2], while a single gene (*itpr*) codes for DmInsP₃R in the *Drosophila* genome [3,4]. All 3 mammalian isoforms share a common domain structure and 60–70% sequence identity [2]. InsP₃Rs are subjected to multiple levels of regulation [1,5,6]. The structural determinants responsible for InsP₃R1 conductance and gating properties [7,8] and modulation by Ca²⁺ [9–11], ATP [12] and phosphorylation [13] have been uncovered in recent functional experiments with InsP₃R1 wild-type and mutant channels.

The *Drosophila* InsP₃R protein (DmInsP₃R) shares the same domain structure and ~60% sequence identity with mammalian InsP₃R isoforms (reviewed in [14]), with the highest level of conservation in the amino-terminal ligand binding and the carboxy-terminal channel regions. Recently, single channel properties of the *Drosophila* wild-type isoforms and two single point mutants (*wc703* and *ug3*) identified in a genetic screen have been described [15,16]. An additional mutant identified in genetic screen (*ka901*) contains a single point mutation in a putative pore-forming region of the DmInsP₃R. Expression of full-length *ka901* mutant in Sf9 cells did not result in InsP₃-gated channels in bilayers, indicating that *ka901* homomeric channels are not functional [15]. To analyze *ka901* functional properties, here we investigated functional properties of heteromeric WT:*ka901* channels formed by co-infection of wild-type (WT) DmInsP₃R and *ka901* viruses into Sf9 cells. The observed results provide a novel information about structural determinants of DmInsP₃R pore and explanation to the gain-of-function phenotype observed in *ka901/+* mutant flies.

2. Materials and methods

2.1. Expression of DmInsP₃R in Sf9 cells

Generation of DmInsP₃R wild-type and *ka901* recombinant baculovirus has been previously described [15]. Equal amounts of DmInsP₃R and *ka901* baculovirus were used for co-infection in *Spo-doptera frugiperda* (Sf9) cells as previously described [15]. Expression of DmInsP₃R and *ka901* isoforms in Sf9 cells was confirmed by Western blotting with the affinity purified anti-DmInsP₃R rabbit polyclonal antibody (IB-9075) that was previously described [15].

2.2. Single channel recordings and analysis of DmInsP₃R activity

Recombinant DmInsP₃R channels expressed in Sf9 cells were incorporated into the bilayer by microsomal vesicle fusion as previously described [10,12,15]. The *cis* chamber contained 250 mM HEPES-Tris, pH 7.35, and the *trans* chamber, which was held at virtual ground, contained 55 mM Ba(OH)₂ dissolved in 250 mM HEPES, pH 7.35. Single-channel conductance values of heteromeric *ka901* channels were determined from the slope of a linear fit to unitary current amplitude versus transmembrane voltage data in the range between +10 and –30 mV.

3. Results

The domain structure of the InsP₃R [2] is conserved between DmInsP₃R and mammalian InsP₃R isoforms. The *ka901* mutation (G2630S) described in earlier studies [15,16] resides

* Corresponding author. Fax: +214-648-2974.

E-mail address: Ilya.Bezprozvanny@UTSouthwestern.edu (I. Bezprozvanny).

Abbreviations: DmInsP₃R, *Drosophila melanogaster* inositol 1,4,5-trisphosphate receptor; WT, wild-type; RyanR, ryanodine receptor

in a carboxy-terminal channel-forming domain of DmInsP₃R. G2630 residue mutated in ka901 is located within a putative pore-forming region and highly conserved within InsP₃R and RyanR gene families and in a region homologous to the selectivity filter of K⁺ channel family (Fig. 1). Flies with one copy of ka901 mutation and a deficiency for the InsP₃R (*itpr*^{90B0}) die as second instar larvae [16], similar to the homozygous deficiency (*itpr*^{90B0}/*itpr*^{90B0}) [17], indicating that in homozygous state ka901 mutation behaves similar to the loss of function mutation. Consistent with this conclusion, ka901 mutants expressed in Sf9 cells by baculovirus infection failed to form functional channels in bilayers [15]. In contrast to these results, Ca²⁺ release experiments with microsomal vesicles extracted from adult heads of ka901/+ heterozygotes showed over twofold higher calcium release as compared to wild-type [15], indicative of a gain-of-function phenotype.

To explain the discrepancy between ka901/ka901 and ka901/+ phenotypes, we reasoned that ka901 forms functional channels only when assembled with the wild-type (WT) DmInsP₃R subunits, but not in the homomeric state. To test this prediction and to examine the functional properties of WT:ka901 channels, we co-expressed ka901 and DmInsP₃R subunits in Sf9 cells at 1:1 ratio by baculovirus co-infection. The expression levels of WT:ka901 channels in Sf9 cells were similar to the wild-type DmInsP₃R and ka901 subunits expressed in isolation (Fig. 2).

In contrast to experiments with ka901 microsomes [15], InsP₃-gated channels were observed routinely (in 13 out of 18 experiments) in bilayer experiments with WT:ka901 microsomes. In three out of 18 experiments, the properties of observed channels were similar to the wild-type DmInsP₃R (data not shown), and we reasoned that these channels result from WT homotetramers. However, in 10 out of 18 experiments the conductances and gating properties of the observed channels (Fig. 3B) were clearly distinct from the wild-type DmInsP₃R.

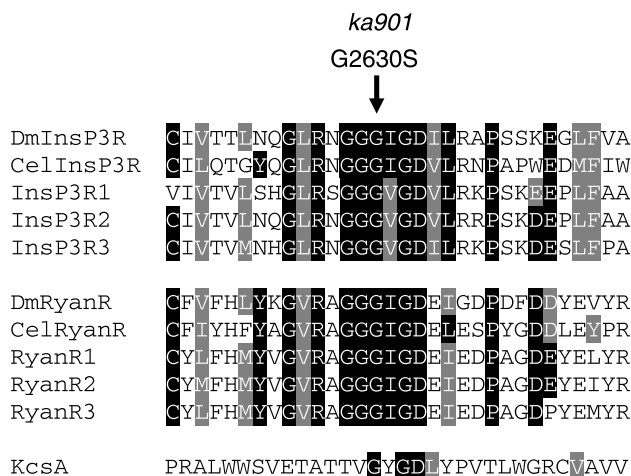


Fig. 1. Sequence alignment of the putative pore regions of InsP₃R and RyanR gene families with the KcsA potassium channel. Amino acid sequence of the putative pore regions of the *Drosophila* InsP₃R (DmInsP₃R), *C. elegans* InsP₃R (CelInsP₃R), mammalian InsP₃R1, InsP₃R2, InsP₃R3, *Drosophila* RyanR (DmRyanR), *C. elegans* RyanR (CelRyanR), mammalian RyanR1, RyanR2, RyanR3, and bacterial potassium channel (KcsA). Residues with 50% sequence identity (black) or similarity (grey) are colored by BoxShade. The arrow shows the G2630 residue mutated in ka901 [15,16].

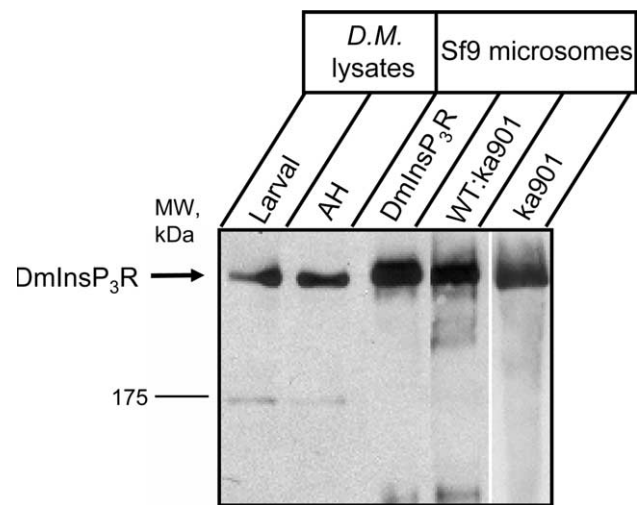


Fig. 2. Expression of WT:ka901 heteromeric channels in Sf9 cells. Western blot of *Drosophila* larval and adult head (AH) lysates and microsomes isolated from Sf9 cells infected with DmInsP₃R, WT:ka901 and ka901 baculoviruses as indicated. The DmInsP₃R was detected using an affinity purified anti-DmInsP₃R polyclonal antibody. For the larval lysate 30 µg of total protein was loaded, while 20 µg was loaded in the lane containing the adult head lysate. For each microsomal preparation, 100 ng of total microsomal protein was loaded on the gel.

We reasoned that these channels are formed by WT:ka901 heteromers. Although exact stoichiometry of these heteromers in the bilayers is unknown, the frequency of these channels' occurrence indicates that the presence of a single ka901 subunit in a tetramer is sufficient to change DmInsP₃R gating and conductance properties (see Section 4). Only heteromeric WT:ka901 channels were considered in the following analysis.

The mean current amplitude of WT:ka901 channels at 0 mV holding potential is equal to 1.87 ± 0.03 pA ($n = 4$) with a mean open dwell time of 6.2 ± 0.5 ms (Fig. 3B). In the same recording conditions, WT DmInsP₃R display unitary current amplitude of 1.8 pA and mean open dwell time of 4.3 ms [15]. Thus, unitary current is increased by 4% and mean open time is increased by 44% in the presence of ka901 subunit. In contrast to DmInsP₃R, WT:ka901 channels displayed a sub-conductance state with amplitude of 70% of the open state (Fig. 3B) in about 25% of the channel openings. This sub-conductance state was found to be a property of a single hybrid channel, as transitions between open and sub-conductance states were observed in membranes with only a single functional channel. The presence of a single functional tetramer in the bilayer was deduced by the amplitude of channel opening observed over 10–30 min. In cases where more than one functional channel is present in the bilayer, some openings have amplitudes which are greater than that of the single channel opening.

Single-channel conductances of 86.0 ± 0.2 pS and 39.0 ± 0.1 pS were estimated for the open and sub-conductance states, respectively (Fig. 4), as compared with the 70.0 ± 0.1 pS conductance of the WT DmInsP₃R (Fig. 4) [15]. Extrapolation of the current-voltage curve to the intercept on the voltage axis indicated a -18 mV shift of approximated reversal potential for the *I/V* curve of the full-open state of the WT:ka901

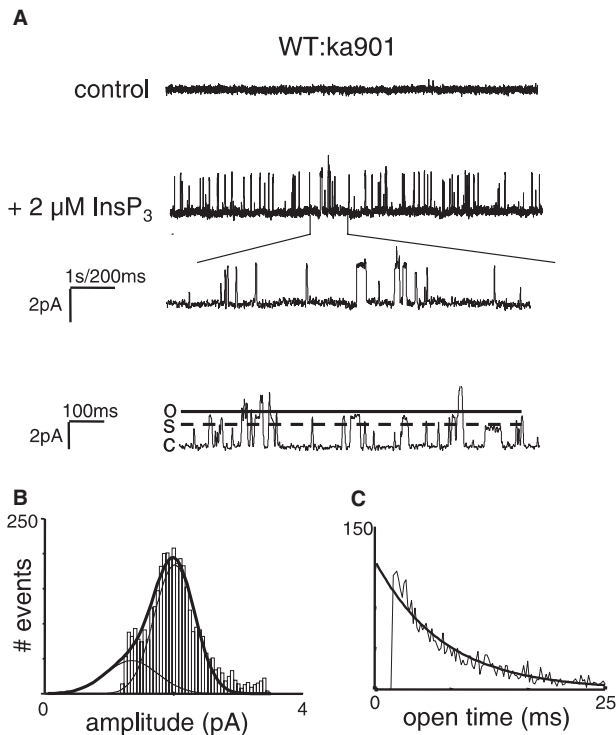


Fig. 3. Functional properties of WT:ka901 channels. (A) Representative channel activity of WT:ka901 channels recorded in the *standard recording conditions*. Current records are shown at compressed and expanded time scales as indicated. Full open state (o) and subconductance state (s) levels are indicated on the expanded record. Unitary current amplitude histograms and open dwell time distributions from the same experiments are shown below the current records. (B) Unitary current distribution was fitted (bold line) with the sum of two Gaussian functions (thin lines), which were centered at 2.0 pA for the full open state and 1.34 pA for the subconductance state. Open time distributions for a full open state were fit with a single exponential function (curve) that yielded a τ_0 of 7.4 ms. Similar analysis was performed for at least four independent experiments with WT:ka901 microsomes.

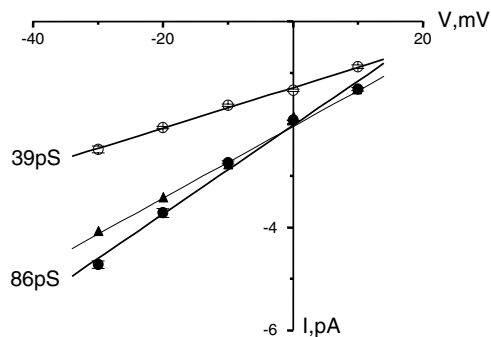


Fig. 4. Current–voltage relationship of ka901:WT heteromeric channels. Current–voltage relationship of the full open state (filled circles) and subconductance state (open circles) of WT:ka901 channels measured at transmembrane voltages between +10 and –30 mV. The average data from at least three independent experiments are shown as means \pm S.E.M at each voltage. The linear fit to the data (thick lines) yielded single channel conductance of 86 pS for full open state and 39 pS for the subconductance state of WT:ka901 channels. The current–voltage relationship of the wild-type DmInsP₃R (embryonic form, filled triangles) from [15] is also shown (thin line). Extrapolation of current–voltage relationships of WT:ka901 and DmInsP₃R channels yielded extrapolated reversal potential equal to +24 mV for full open state of WT:ka901 channels, +50 mV for the subconductance state and +42 mV for the wild-type DmInsP₃R channels.

channels when compared to wild-type channels (Fig. 4). Since 55 mM Ba²⁺ in the trans chamber is the sole current carrier in the system, this change in reversal potential in the mutant indicates an alteration in ion selectivity of the heteromeric WT:ka901 channel.

The observed effects on single-channel conductance, selectivity and channel gating are consistent with the position of the ka901 mutation (G2630S) in the pore region of DmInsP₃R (Fig. 1). In additional experiments, we determined the Ca²⁺-sensitivity of WT:ka901 channels. Firstly, the presence of only heteromeric channels in the bilayer was confirmed by measuring current–voltage relationship as described above (Fig. 4). Subsequently, calcium dependence experiments were carried out with the same bilayer. We observed that the bell-shaped Ca²⁺-dependence of the WT:ka901 channels was similar to that of the wild-type DmInsP₃R [15] (data not shown), suggesting that DmInsP₃R modulation by Ca²⁺ is not influenced by the ka901 mutation.

4. Discussion

The absence of functional channels from ka901 homomers in bilayer experiments [15] agrees with the genetic finding that the allelic strength of ka901 is equivalent to that of the null allele *itpr*^{90B0} [16]. However, when co-expressed with the wild-type DmInsP₃R, ka901 mutant behaves as a “gain of function” mutant in the vesicle flux assay [15]. As shown here, these results can be explained by increasing single-channel conductance (23% increase) and open dwell time (44% increase) of heteromeric WT:ka901 DmInsP₃R channels. These effects on conductance and gating properties of DmInsP₃R are consistent with the position of ka901 mutation (G2630S) within the predicted pore-forming region of DmInsP₃R (Fig. 1). The pore-forming regions of InsP₃R and RyanR families are highly conserved and contain a putative pore-forming motif GXRXGGGGI/VGD (the G2630 residue of DmInsP₃R mutated in ka901 is underlined). The G4826 residue in RyanR2 is homologous to the G2630 residue mutated in ka901. Mutation studies of this residue revealed conductance properties that support our observations in ka901 [18,19]. The G4826C mutant does not form functional homomeric channels in bilayer experiments [19], similar to what we observe with ka901 homomeric channels. Co-transfection studies of G4826C with wild-type RyanR2 showed the presence of a single type of hybrid channel and not four types of hybrid channels, as seen in the case of the G4824A mutant and RyanR2 co-transfections [18,19]. Interestingly, similar to our observation of increase in conductance of WT:ka901 hybrid channels, the conductance of the full open state of WT:G4826C hybrid channels is also increased by ~25% when compared with RyanR2. The exact subunit composition of heteromeric channels is not known for either WT:ka901 DmInsP₃R (Figs. 3 and 4) or WT:G4826 RyanR2 [19]. The observation of a single sub-conductance state and a single full-open state indirectly suggests that some hybrid channels may not be functional. Thus, properties of WT:ka901 DmInsP₃R channels mirror those of WT:G4826C RyanR2 channels, presumably due to the similarity between the cysteine (CH2-SH) and serine (CH2-OH) side chains found in G4826C and ka901 mutants, respectively. Most likely, the presence of a larger side-chain in

these mutants in narrow selectivity filters of DmInsP₃R or RyanR2 channels puts a limit on a number of mutant subunits in a functional channel. The presence of a single sub-conductance state indicates the presence of only one functional heteromer. Multiple sub-conductance states were observed in case of the G4824A mutant of RyanR2, which indicated the stoichiometry of wild-type and mutant channels in the tetramer [18]. Similarly, we reasoned that the presence of different sub-conductance states would indicate the presence of multiple heteromers in different stoichiometries. Instead, we observed only a single sub-conductance state. Since a tetramer consisting of four ka901 subunits does not form functional channel [15], we reason that the most likely functional tetramer would comprise 3WT and 1 ka901 subunits. An alternate stoichiometry is also possible.

Increase in conductance of the single functional state in WT:ka901 DmInsP₃R (Fig. 4) or WT:G4826 RyanR2 [19] may arise from an interaction of the side chain (either -OH or -SH) with the back bone. The idea of an interaction between the side chain and the backbone is supported by another study, of the I4898T mutation of RyanR1, which has been linked to central core disease [20]. The I4898 position in RyanR1 corresponds to the isoleucine residue in the GGGI/VGD putative pore-forming motif of RyanR and InsP₃R, and thus lies adjacent to the G residue mutated in ka901. It has been shown that RyanR channels are leaky in cells co-transfected with WT RyanR1 and I4898T mutants [20]. Similar to our findings with ka901, homomeric tetramers of the I4898T mutant of RyanR1 are non-functional as judged by Ca²⁺ photometry experiments [20]. Consistent with our observations of ka901 channels, it seems likely that the leaky channel arises from an interaction of the -OH (in the threonine side chain) with the backbone, while in the mutant homotetramer the pore is blocked. Overall, these results highlight the importance of the putative pore-forming motif for ion conductance by InsP₃R and RyanR channels. These results also agree with previous analysis of InsP₃R1 [7,8] pore forming mutants and with the known structure of the potassium channel selectivity filter, which is composed of a similar sequence [21]. In summary, our results demonstrate the conserved function of the G2630 residue in InsP₃R and RyanR Ca²⁺ channel families.

Acknowledgements: S.S.'s visit to Dallas was supported by J. Cell Science travelling fellowship. I.B. is supported by the Robert A. Welch Foundation and NIH R01 NS38082. G.H. is supported by a grant from the Department of Science and Technology and core grants from the National Centre for Biological Sciences, TIFR, Bangalore.

References

- [1] Berridge, M.J. (1993) *Nature* 361, 315–325.
- [2] Furuichi, T., Kohda, K., Miyawaki, A. and Mikoshiba, K. (1994) *Curr. Opin. Neurobiol.* 4, 294–303.
- [3] Hasan, G. and Rosbash, M. (1992) *Development* 116, 967–975.
- [4] Yoshikawa, S., Tanimura, T., Miyawaki, A., Nakamura, M., Yuzaki, M., Furuichi, T. and Mikoshiba, K. (1992) *J. Biol. Chem.* 267, 16613–16619.
- [5] Bezprozvanny, I. and Ehrlich, B.E. (1995) *J. Membr. Biol.* 145, 205–216.
- [6] Taylor, C.W. (1998) *Biochim. Biophys. Acta* 1436, 19–33.
- [7] Ramos-Franco, J., Galvan, D., Mignery, G.A. and Fill, M. (1999) *J. Gen. Physiol.* 114, 243–250.
- [8] Boehning, D., Mak, D.O., Foskett, J.K. and Joseph, S.K. (2001) *J. Biol. Chem.* 276, 13509–13512.
- [9] Miyakawa, T., Mizushima, A., Hirose, K., Yamazawa, T., Bezprozvanny, I., Kurosaki, T. and Iino, M. (2001) *EMBO J.* 20, 1674–1680.
- [10] Nosyreva, E., Miyakawa, T., Wang, Z., Glouchankova, L., Mizushima, A., Iino, M. and Bezprozvanny, I. (2002) *Biochem. J.* 365, 659–667.
- [11] Tu, H., Nosyreva, E., Miyakawa, T., Wang, Z., Mizushima, A., Iino, M. and Bezprozvanny, I. (2003) *Biophys. J.* 85, 290–299.
- [12] Tu, H., Miyakawa, T., Wang, Z., Glouchankova, L., Iino, M. and Bezprozvanny, I. (2002) *Biophys. J.* 82, 1995–2004.
- [13] Tang, T.S., Tu, H., Wang, Z. and Bezprozvanny, I. (2003) *J. Neurosci.* 23, 403–415.
- [14] Srikanth, S. and Hasan, G. (2004) *Curr. Sci.* 86, 1513–1523.
- [15] Srikanth, S., Wang, Z., Tu, H., Nair, S., Mathew, M.K., Hasan, G. and Bezprozvanny, I. (2004) *Biophys. J.* 86, 3634–3646.
- [16] Joshi, R., Venkatesh, K., Srinivas, R., Nair, S. and Hasan, G. (2004) *Genetics* 166, 225–236.
- [17] Venkatesh, K. and Hasan, G. (1997) *Curr. Biol.* 7, 500–509.
- [18] Zhao, M., Li, P., Li, X., Zhang, L., Winkfein, R.J. and Chen, S.R. (1999) *J. Biol. Chem.* 274, 25971–25974.
- [19] Chen, S.R., Li, P., Zhao, M., Li, X. and Zhang, L. (2002) *Biophys. J.* 82, 2436–2447.
- [20] Lynch, P.J. et al. (1999) *Proc. Natl. Acad. Sci. USA* 96, 4164–4169.
- [21] Doyle, D.A., Morales Cabral, J., Pfuetzner, R.A., Kuo, A., Gulbis, J.M., Cohen, S.L., Chait, B.T. and MacKinnon, R. (1998) *Science* 280, 69–77.